

Project 1 - Monte Carlo

Authors goes here

I. INTRODUCTION

The GitHub repository is available here: <https://github.com/Caronthir/FYSSTK4155/projects/>.

$$\langle x \rangle = \int_{\mathbb{R}} xp(x)dx \approx \frac{1}{M} \sum_{i=1}^M x_i p(x_i)$$

Applying this to an observable \mathcal{O} , we have

II. THEORY

A. Variational Monte Carlo

In order to find a good candidate wavefunction for a given potential, one can employ the *variational principle*. One starts by guessing a trial wavefunction $|\Psi_T\rangle$ and estimating the trial energy, which is guaranteed to be equal to or higher than the true ground state energy E_0 :

$$E_0 \leq E = \frac{\langle \Psi_T | H | \Psi_T \rangle}{\langle \Psi_T | \Psi_T \rangle} \quad (\text{II.1})$$

If $|\Psi_T\rangle$ is an eigenfunction of the Hamiltonian, the variance σ^2 will be minimal

$$\sigma^2 = \frac{\langle \Psi_T | H^2 | \Psi_T \rangle}{\langle \Psi_T | \Psi_T \rangle} - \left(\frac{\langle \Psi_T | H | \Psi_T \rangle}{\langle \Psi_T | \Psi_T \rangle} \right)^2 = 0$$

The variational principle expands on this idea by letting $|\Psi_T\rangle$ be a functional class of a *variational parameter* α . By varying α one can find the optimal trial wavefunction within the functional class by minimizing σ^2 .

Only a small collection of potentials have analytical solution using the variational principle. For most potentials, one must numerically integrate (II.1) using Monte Carlo integration.

For a stochastic variable x with probability density function $p(x)$, the average $\langle x \rangle$ is defined as

$$\langle x \rangle = \int_{\mathbb{R}} xp(x)dx$$

By sampling the stochastic variable M times, the average can be approximated by

$$\begin{aligned} \langle \mathcal{O} \rangle &= \langle \Psi | \mathcal{O} | \Psi \rangle \\ &= \int d\mathbf{r} \Psi^* \mathcal{O} \Psi \\ &= \int d\mathbf{r} |\Psi|^2 \frac{1}{\Psi} \mathcal{O} \Psi \\ &= \frac{1}{M} \sum_{i=1}^M p(\mathbf{r}) \mathcal{O}_L \end{aligned}$$

where $|\Psi|^2$ is defined as the probability density function, and $\frac{1}{\Psi} \mathcal{O} \Psi$ the *local operator*.

The local trial energy can then be defined as

$$E_L = \frac{1}{\Psi_T} H \Psi_T$$

which can be computed using Monte Carlo integration as

$$\langle E_L \rangle \approx \frac{1}{M} \sum_{i=1}^M p(\mathbf{r}_i) E_L(\mathbf{r}_i)$$

The goal is therefore to minimize minimizing $\sigma^2 = \langle E_L^2 \rangle - \langle E_L \rangle^2$ over the variational parameter α .

B. Gradient Descent

The optimal value for the variational parameter is found by gradient descent.

C. The System

1. The Potentials

The Hamiltonian under investigation describes N bosons in a potential trap, and is on the form

3. Non-interacting Case

$$H = \sum_{i=1}^N \left(\frac{-\hbar^2}{2m} \nabla_i^2 + V_{\text{ext}}(\mathbf{r}_i) \right) + \sum_{i<j}^N V_{\text{int}}(\mathbf{r}_i, \mathbf{r}_j)$$

where V_{ext} is the external potential of the trap while V_{int} is the internal potential between the particles. The external potential has an elliptical form, being anisotropic in the z -direction:

$$V_{\text{ext}}(\mathbf{r}) = \frac{1}{2}m(\omega[x^2 + y^2] + \omega_z z^2) \quad (\text{II.2})$$

The internal potential is a hard shell potential, being infinite for distances where two bosons overlap:

$$V_{\text{int}} = \begin{cases} \infty, & \text{for } |\mathbf{r}_i - \mathbf{r}_j| \leq 0 \\ 0, & \text{otherwise} \end{cases}$$

2. The Trial Wavefunction

The elliptical spherical trap (II.2) represents a harmonic oscillator. As the trial wavefunction should be as close as possible to the expected true wavefunction, a reasonable guess at its shape is the eigenfunction of harmonic oscillators, namely Gaussian functions. For a N -bosonic system the trial wavefunction is therefore

$$\begin{aligned} h(\mathbf{r}_1, \dots, \mathbf{r}_N, \alpha, \beta) &= \prod_{i=1}^N g(\mathbf{r}_i, \alpha, \beta) \\ &= \exp \left\{ - \sum_{i=1}^N (x_i^2 + y_i^2 + \beta z_i^2) \right\} \end{aligned}$$

with g the onebody function. The internal potential should cause the wavefunction to decrease continuously down to zero as the distance of two particles goes to zero. Once such possible function is

$$f(a, \mathbf{r}_i, \mathbf{r}_j) = \begin{cases} 0, & |\mathbf{r}_i - \mathbf{r}_j| \leq a \\ 1 - \frac{a}{|\mathbf{r}_i - \mathbf{r}_j|}, & \text{otherwise} \end{cases}$$

Combining both potential contributions, the complete trial wave function is therefore

$$\Psi_T(\mathbf{r}, \alpha, \beta, a) = \exp \left\{ -\alpha \sum_{i=1}^N (x_i^2 + y_i^2 + \beta z_i^2) \right\} \prod_{i<j}^N f(a, \mathbf{r}_i, \mathbf{r}_j)$$

For non-interacting bosons in a spherical with $\beta = 1$ and $a = 0$ the system reduces to spherical harmonic oscillators where analytical solutions are available. The trial wavefunction reduces to simply the product of one body elements

$$\Psi_T(\mathbf{r}) = \prod_i^N \exp[-\alpha(x_i^2 + y_i^2 + z_i^2)] = \prod_i^N \exp(-\alpha|\mathbf{r}_i|^2)$$

while the Hamiltonian reduces to

$$H = \sum_i^N \frac{-\hbar^2}{2m} \nabla_i^2 + \frac{1}{2}m\omega^2 r_i^2$$

which in natural units is

$$H = \frac{1}{2} \sum_i^N -\frac{1}{m} \nabla_i^2 + m\omega^2 r_i^2$$

Applying the Hamiltonian gives the local energy as

$$E_L = \frac{\alpha d}{m} N + \left(\frac{1}{2}m\omega^2 - \frac{2\alpha^2}{m} \right) \sum_i^N r_i^2$$

where d is the dimension. As the factor $\sum_i^N r_i^2$ is always positive, its term should be minimized, which is accomplished by setting $\alpha = \frac{m\omega}{2}$, giving a minimal local energy of

$$E_L = \frac{\omega d N}{2} \quad (\text{II.3})$$

4. Interacting Case

The local energy for the full interacting case is much more complicated. The full computation is deferred to appendix A.

D. Drift Force

E. Onebody Density

III. METHOD

A. Outline of Program

B. Non Interacting Potentials

C. Interacting Potentials

D. Statistical Treatment

IV. RESULTS

A. Non Interacting Potentials

B. Interacting Potentials

C. Local Energy

D. Optimal Parameter α

E. Onebody Density

V. RESULTS AND DISCUSSION

A. Validating the Model

| N | Numerical | Analytical |
|-----|-----------|------------|
| 1 | | |
| 2 | | |
| 10 | | |
| 100 | | |

Table V.1: Non-interactive particles in spherical potential compared to analytical solution for $\alpha = 0.5$. By (II.3), there is not spatial dependency, making the comparison easy.

To validate that our implementation works correctly, the model is run for a spherical potential without any interactions. The expected local energy is compared to the analytical solution, summarized in table V.1. The computed energies are exactly $\frac{d}{2}$ of the number of particles, as expected from Equation (II.3) on the previous page.

Further validation is performed by comparing the one body density found from brute force sampling, importance sampling and analytical solution REF TO EQ, shown in fig. V.1. Aside from the statistical noise introduced by the finite number of Monte-Carlo cycles, the approximated densities follow the analytical result closely. Figure V.2 demonstrates how this scales with more particles and dimensions, as seen from the

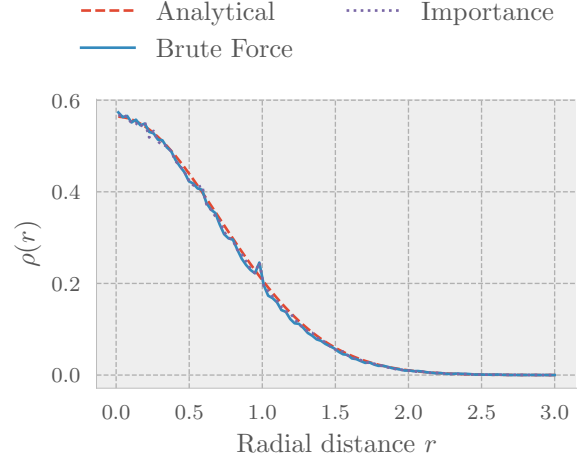


Figure V.1: One-body density of 1 boson in 1 dimension, using $N = 1e6$ cycles, $\omega = 1$, $\alpha = 0.5$.

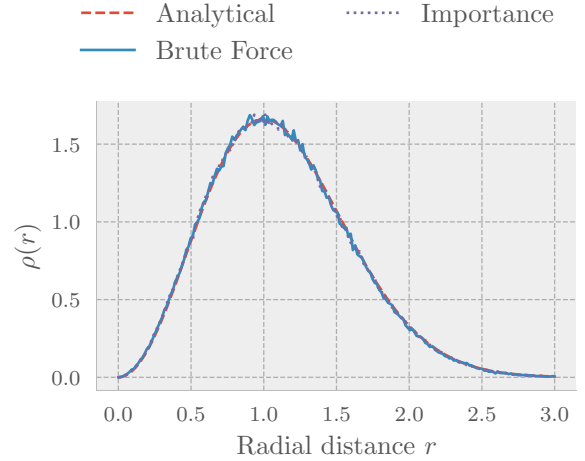


Figure V.2: Radial one-body density of 2 non-interacting bosons in 3 dimensions, using $N = 1e6$ cycles, $\omega = 1$, $\alpha = 0.5$.

radial onebody density of two particles in three dimensions.

B. Blocking of Local Energy

The effect of applying blocking to the local energy before calculating the variance is shown in fig. V.3. Although the local energies are sampled from an approximately correct distribution, the data is produced by moving a single boson at a time. The move may be rejected by the metropolis algorithm, causing no change in state. Because of this, the data is highly correlated, leading to an underestimation of the vari-

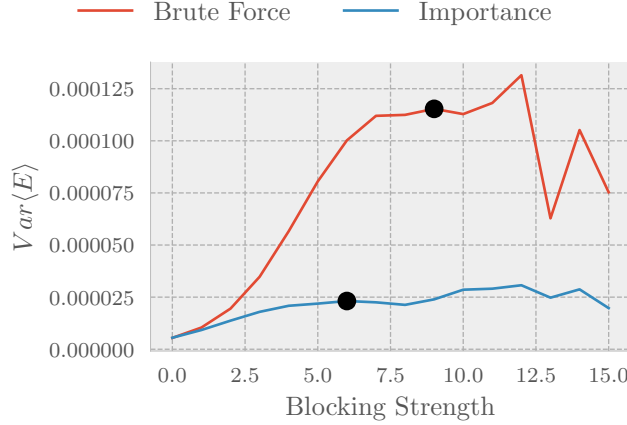


Figure V.3: Variance of the estimate of $\langle E_L \rangle$ using blocked values of local energy at various strengths. As the blocking strength increases, the autocorrelation is decreased and variance increases before it plateaus, shown with the black dot. The data have been produced for 40 non-interacting bosons in three dimensions using $N = 2^{20}$ cycles, $\alpha = 0.8$, $\omega = 1$, with and without importance sampling

| dt | $\langle E \rangle$ | blocking strength |
|-----|---------------------|-------------------|
| 0.5 | 68.009 ± 0.044 | 11 |
| 1 | 68.039 ± 0.035 | 10 |
| 2 | 67.942 ± 0.050 | 11 |

Table V.2: Estimate of energy $\langle E \rangle$ for 40 particles, $\alpha = 0.3$, $\omega = 1$

ance as seen for the unblocked data. The variance stabilizes after repeated blocking, when the data is approximately uncorrelated. Note that this happens at different strength for brute force sampling and importance sampling. From [fig. V.3](#) the latter requires a weaker blocking strength, indicating that the data created are less correlated. This is expected as importance sampling uses additional information from the wave function and explores the space of states more efficiently than brute force. The variance stabilizes at strength 6 when using importance sampling as opposed to 9 when using brute force. This grants eight times the effective amount of data and thus a smaller variance of the estimator.

The effect of blocking for a larger system is shown in [fig. V.4](#) using only importance sampling and step lengths of 0.5, 1 and 2. As only a single particle is moved in each MC cycle, increasing the size of the system results in a comparatively smaller change. The local energies will invariably become more correlated, which is apparent when comparing the blocking strengths from [fig. V.4](#) to [fig. V.3](#).

Further, the least correlated data was produced for a step length of $\delta t = 1$, requiring blocking strength 10 as opposed to 11 for $\delta t = 0.5$ and 2. Using a step length too small results in the local energy changing minimally

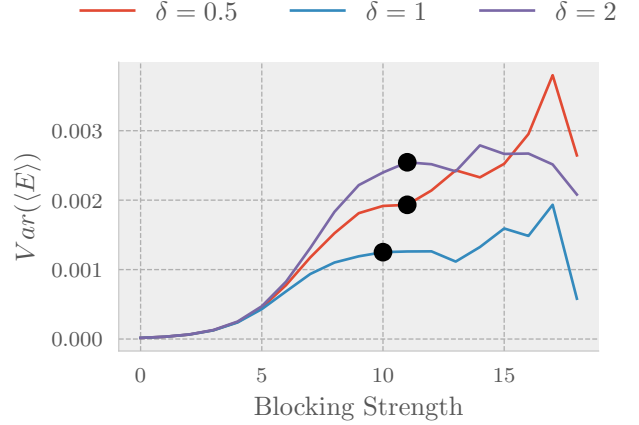


Figure V.4: Variance of the estimate of $\langle E \rangle$ using blocked values of local energy at various strengths. The data has been produced for 40 non-interacting bosons in 3 dimension, using $N = 2^{20}$ cycles, $\alpha = 0.8$, $\omega = 1$, using importance sampling with step length 0.5, 1 and 2, respectively

from cycle to cycle, increasing the correlation and minimizing the effective amount of data. The same happens if the step length is too big, as large moves will tend to be rejected often, causing repeated values to be sampled. [Table V.2](#) presents the resulting estimates of energy with the uncertainty established using the blocking. The estimated energy is only sensitive to the step length in the sense that more cycles may be needed to get an accurate result of the step length is taken too small or too big.

C. Energy of Non-Interacting System

Varying the variational parameter α gives different trial wave functions that have different expected local energy. For the non-interacting spherical system there are analytical solutions for the α -dependency of the local energy, and can be used to validate our model. This comparison is shown in [fig. V.5](#) and [fig. V.6](#). The curves overlap within the MC-uncertainty as expected, with the minimum occurring at $\alpha = 0.5$, giving confidence in the implementation.

D. Numerical and Analytical Laplacian

When evaluating the Hamiltonian, one can choose to use the analytical expression for the Laplacian or compute it numerically using finite differences. Both methods give the same solution, as illustrated by [fig. V.7](#). Suspecting that the computational cost differs, their CPU time are plotted in [fig. V.8](#). The difference is negligible with few particles, but the numerical Laplacian

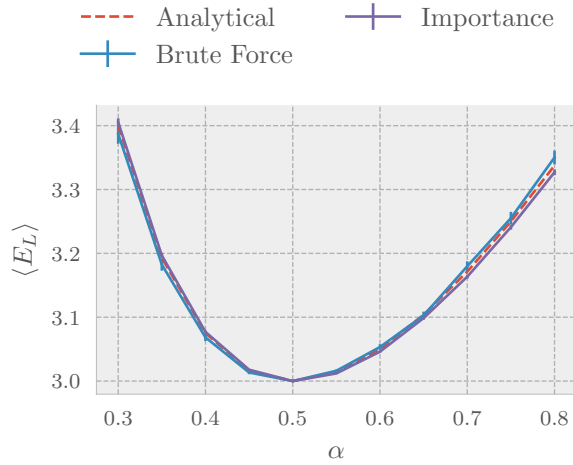


Figure V.5: The expected local energy as function of the variational parameter α for both brute force and importance sampling, compared to the analytical solution. The system consists of two non-interacting bosons using 2^{17} cycles.

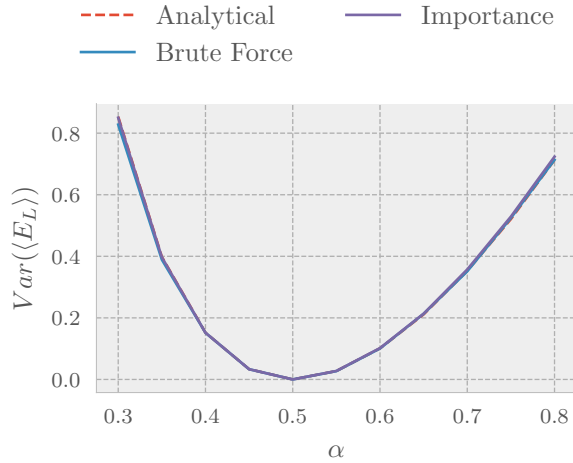


Figure V.6: The variance of the expected local energy as function of the variational parameter α for both brute force and importance sampling, compared to the analytical solution. The system consists of two non-interacting bosons using 2^{17} cycles.

quickly outgrows the analytical, showing exponential dependency on the number of particles. Most potentials do now have analytical solution, having to rely on the much slower numerical computation.

E. Interacting Potentials

Adding interaction between the bosons drastically changes the behavior of the system. In [fig. V.9](#) non-interacting bosons are compared to systems having two

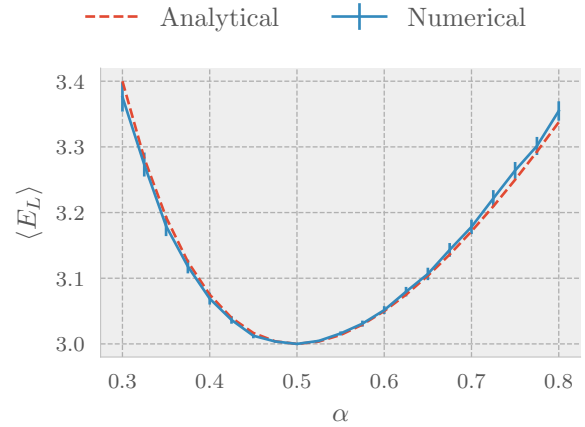


Figure V.7: Estimated energy $\langle E_L \rangle$ for two non-interacting bosons, comparing the analytical solution to numerically evaluated Laplacian. 2^{17} cycles, $\omega = 1$ and importance sampling was used. Errorbars were established using blocking.

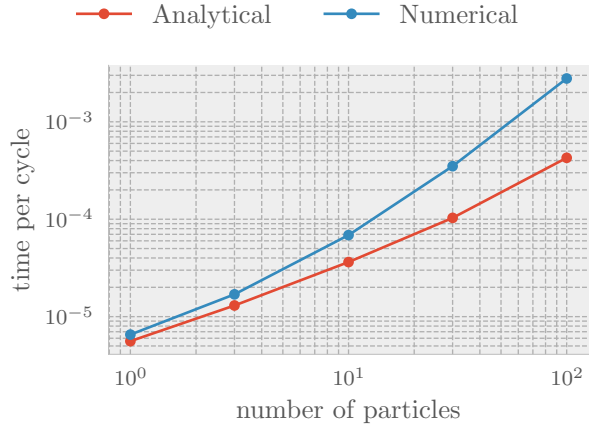


Figure V.8: Comparison of CPU-time of numerical and analytical Laplacian for different numbers of particles. The timing is with respect to the whole simulation, including writing to file. However, as the uninteresting steps are of $\mathcal{O}(1)$, they are irrelevant when comparing the graphs.

and three interacting bosons. The densities the latter are spread out, with maxima directly proportional to the number of particles. The interpretation is that the interacting particles are repelled by each other and attempts to minimize their energy while staying within the potential, resulting in N bumps becoming more and more spread out as N grows.

F. Optimal Parameter α

Gradient descent was performed on the variational parameter α with non-interactive bosons. [Figure V.10](#)

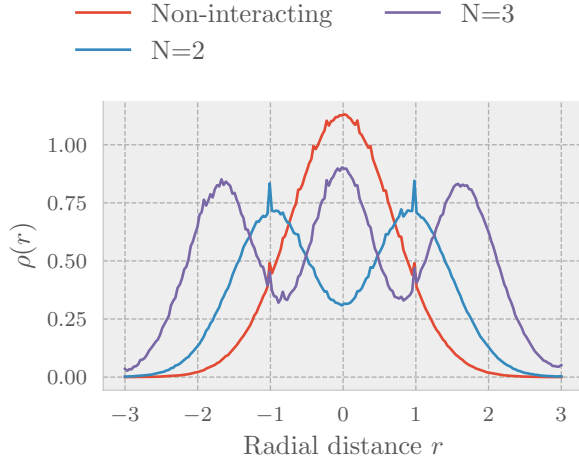


Figure V.9: One body density ρ in one dimension for two non-interacting bosons, two interacting bosons, and three interacting bosons. Non-interacting bosons occupies the same space to minimize the energy, while the interacting bosons separate. The more bosons, the greater they spread out.

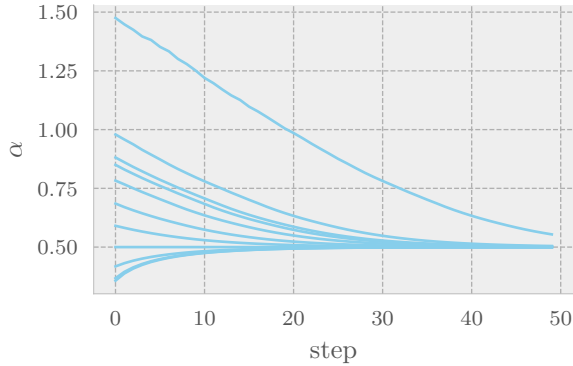


Figure V.10: Gradient decent on the parameter α for two non-interacting bosons with different α_0 , learning rate $\mu = 0.01$, $N = 10000$ steps and $\omega = 1$

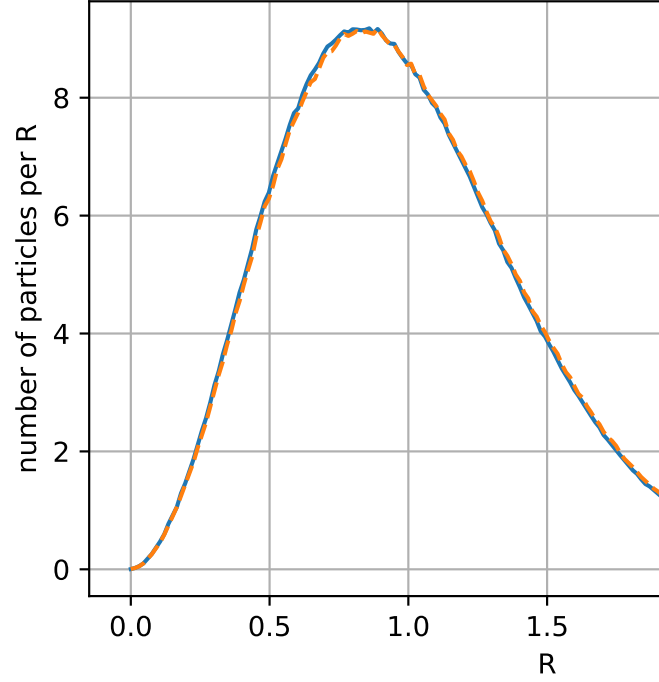
shows the results. The method is robust for different initial guesses α_0 , all converging to 0.5 as expected. This establishes confidence that the method will converge to the optimal α in the interacting case where the analytical solution is not known.

G. Interacting Bosons in Elliptical Potential

Table V.3 presents the estimated ground state energies for 10, 50 and 100 interacting bosons confined by a elliptical potential. The optimal value for α was found using gradient decent. Notice that the optimal value

| Bosons | $\langle E \rangle$ | optimal α |
|--------|----------------------|------------------|
| 10 | 24.3985 ± 0.0011 | 0.49752 |
| 50 | 127.37 ± 0.035 | 0.48903 |
| 100 | 265.69 ± 0.27 | 0.48160 |

Table V.3: Estimate of energy $\langle E \rangle$ for 10, 50 and 100 particles in elliptical potential. $\beta = \gamma = 2.8284$. $N = 2^{20}$ cycles per thread, of 12 threads. Importance sampling with a step length 0.5 was used. Gradient decent was used to optimize α



(a) Radial onebody density for 10 bosons in elliptical trap, interacting and non-interacting

Figure V.11: Comparison of the radial onebody density for interacting and non-interacting bosons. The hardshell radius of in the interacting case is $\alpha = 0.0043$. The elliptical potential is defined by $\beta = \gamma = 2.82843$.

is decreasing with the number of particles in the interacting case, whereas it is analytically $\alpha = 0.5$ in the non-interacting case for any number of particles. A smaller value of α indicates the onebody exponential functions widens, resulting in a wider distribution of particles. This makes sense, as hardshell bosons interact repulsively. Therefore, the more particles, the more energetically favorable is it to spread out. This is consistent with the 1D result presented in Figure V.11. As the number of particles increase, the radial onebody density tends to migrate outward with respect to the non-interacting system.

The ground state energy was most accurately calculated for 10 bosons. This is because, as discussed earlier, data tend to be less correlated for smaller systems. To get a accurate estimate for larger systems, a increase in the number of cycles is appropriate. How-

ever, because of limited computer power, this was neglected.

A comment on the interpretation of the error presented in Table V.3 is appropriate: The error is an estimate of the statistical error in the estimated ground state energy introduced by the Monte-Carlo simulation. It does not account for possible error introduced in the estimation of α that minimizes the energy. This is much harder to quantify, and is possibly large in the case for 50 and 100 particles, as the gradient was hard to estimate consistently. Furthermore, the error does not in any way establish a confidence interval for the true ground state value of the Hamiltonian we are investigating, which is harder still to quantify. Our estimate a approximate minimum only in the subspace spanned by our trial wave function, which is hopefully, somewhat close the exact solution of the system.

VI. CONCLUSION

Appendix A: Local Energy

1. The Gradient and Laplacian

The full trial wavefunction can be written as

$$\Psi_T(\mathbf{r}) = \prod_i^N \phi(\mathbf{r}_i) \cdot \exp \left(\sum_{j < k} u(r_{jk}) \right)$$

where $u = \ln f(r_{ij})$ and $r_{ij} = |\mathbf{r}_i - \mathbf{r}_j|$.

By the chain rule we can focus on each factor separately when taking the gradient. The gradient of the first factor is simply the gradient of the one body element in question:

$$\nabla_k \prod_i \phi_i = \prod_{i \neq k} \phi_i \cdot \nabla_k \phi_k$$

The second factor is at face value slightly more arduous, but it is trivial. The summation is just a notational trick to ensure that each interaction between all particles are enumerated once and only once. As the gradient only affects particle k , only the interactions involving it will be non-zero. Hence the gradient is

$$\nabla_k \exp \left(\sum_{j < m} u(r_{jm}) \right) = \exp \left(\sum_{j < m} u(r_{jm}) \right) \sum_{l \neq k} \nabla_k u(r_{lk})$$

The total gradient of the trial wavefunction is therefore

$$\begin{aligned} \nabla_k \Psi_T(\mathbf{r}) &= \left[\underbrace{\prod_{i \neq k} \phi_i \cdot \nabla_k \phi_k}_{\text{red dot}} + \underbrace{\prod_i \phi_i \sum_{l \neq k} \nabla_k u(r_{lk})}_{\text{green dot}} \right] \\ &\quad \times \exp \left(\sum_{j < m} u(r_{jm}) \right) \\ &= \left[\frac{\nabla_k \phi_k}{\phi_k} + \sum_{l \neq k} \nabla_k u(r_{lk}) \right] \Psi_T(\mathbf{r}) \quad (\text{A.1}) \end{aligned}$$

The Laplacian is likewise computed termwise

$$\nabla_k^2 \phi_{\text{red}} = \left[\nabla_k^2 \phi \prod_{i \neq k} \phi_i + \nabla_k \phi \sum_{i \neq k} \nabla_k u(r_{ki}) \right] \exp \left(\sum_{j < m} u(r_{jm}) \right)$$

and

$$\begin{aligned} \nabla_k^2 \bullet &= \left[\nabla_k \phi_k \prod_{i \neq k} \phi_i \sum_{l \neq k} \nabla_k u(r_{lk}) \right. \\ &\quad + \prod_i \phi_i \left(\sum_{l \neq k} \nabla_k u(r_{lk}) \right)^2 \\ &\quad \left. + \prod_i \phi_i \sum_{l \neq k} \nabla_k^2 u(r_{lk}) \right] \exp \left(\sum_{j < m} u(r_{jm}) \right) \end{aligned}$$

Combining the results and diving through by Ψ_T then gives

$$\begin{aligned} \frac{\nabla_k^2(\bullet + \bullet)}{\Psi_T} &= \frac{\nabla_k^2 \phi_k}{\phi_k} + \frac{\nabla_k \phi_k}{\phi_k} \sum_{l \neq k} \nabla_k u(r_{lk}) + \frac{\nabla_k \phi_k}{\phi_k} \sum_{l \neq k} \nabla_k^2 u(r_{lk}) \\ &\quad + \left[\sum_{l \neq k} \nabla_k u(r_{lk}) \right]^2 + \sum_{l \neq k} \nabla_k^2 u(r_{lk}) \quad (\text{A.2}) \end{aligned}$$

To compute $\nabla_k u(r_{lk})$, a change of variable is performed, with

$$\nabla_k = \nabla_k(r_{kl}) \frac{\partial}{\partial r_{kl}} = \frac{\mathbf{r}_k - \mathbf{r}_l}{r_{kl}} \frac{\partial}{\partial r_{kl}}$$

and

$$\begin{aligned} \nabla_k \left(\frac{\mathbf{r}_k - \mathbf{r}_l}{r_{kl}} \right) &= \frac{r_{kl} \nabla_k(\mathbf{r}_k - \mathbf{r}_l) - (\mathbf{r}_k - \mathbf{r}_l) \nabla_k r_{kl}}{r_{kl}^2} \\ &= \frac{dr_{kl}^2 - (\mathbf{r}_k - \mathbf{r}_l)(\mathbf{r}_l - \mathbf{r}_k)}{r_{kl}^3} \\ &= \frac{dr_{kl}^2 - \mathbf{r}_k^2 - \mathbf{r}_l^2 + 2\mathbf{r}_k \mathbf{r}_l}{r_{kl}^3} \\ &= \frac{d-1}{r_{kl}} \end{aligned}$$

Applying these relations on (A.2) and multiplying out the squared sum, we obtain the desired result

$$\begin{aligned} \frac{\nabla_k^2 \Psi_T(\mathbf{r})}{\Psi_T(\mathbf{r})} &= \frac{\nabla_k^2 \phi_k}{\phi_k} + 2 \frac{\nabla_k \phi_k}{\phi_k} \left(\sum_{l \neq k} \frac{\mathbf{r}_k - \mathbf{r}_l}{r_{kl}} u'(r_{kl}) \right) \\ &\quad + \sum_{i \neq k} \sum_{j \neq k} \frac{(\mathbf{r}_k - \mathbf{r}_i)(\mathbf{r}_k - \mathbf{r}_j)}{r_{ki} r_{kj}} u'(r_{ki}) u'(r_{kj}) \\ &\quad + \sum_{l \neq k} \left(u''(r_{kl}) + \frac{2}{r_{kl}} u'(r_{kl}) \right) \quad (\text{A.3}) \end{aligned}$$

The full expression involves computing each gradient and derivative. These are found to be

$$\begin{aligned} \nabla_k \phi_k &= -2\alpha \left(x_k \hat{\mathbf{i}} + y_k \hat{\mathbf{j}} + \beta z_k \hat{\mathbf{k}} \right) \phi_k \\ \nabla_k^2 \phi_k &= \left[4\alpha^2 \left(x_k^2 \hat{\mathbf{i}} + y_k^2 \hat{\mathbf{j}} + \beta^2 z_k^2 \hat{\mathbf{k}} \right) - 2\alpha(d-1+\beta) \right] \phi_k \\ u'(r_{ij}) &= \frac{a}{r_{ij}(r_{ij}-a)} \\ u''(r_{ij}) &= \frac{a^2 - 2ar_{ij}}{r_{ij}^2 (r_{ij}-a)^2} \end{aligned}$$

2. The Local Energy

The local energy for the full dimensional interactive case is found by using (A.3) and gradients in

$$E_L = \frac{1}{\Psi_T(\mathbf{r})} H \Psi_T(\mathbf{r})$$

giving

$$\begin{aligned} E_L &= -\frac{1}{2m} \sum_i \left[4\alpha^2 \left(x_k^2 \hat{\mathbf{i}} + y_k^2 \hat{\mathbf{j}} + \beta^2 z_k^2 \hat{\mathbf{k}} \right) \right. \\ &\quad - 2\alpha(d-1+\beta) \\ &\quad - 4\alpha \left(x_k \hat{\mathbf{i}} + y_k \hat{\mathbf{j}} + \beta z_k \hat{\mathbf{k}} \right) \sum_{l \neq k} \frac{\mathbf{r}_k - \mathbf{r}_l}{r_{kl}} u'(r_{kl}) \\ &\quad + \sum_{i \neq k} \sum_{j \neq k} \frac{(\mathbf{r}_k - \mathbf{r}_i)(\mathbf{r}_k - \mathbf{r}_j)}{r_{ki} r_{kj}} u'(r_{ki}) u'(r_{kj}) \\ &\quad \left. + \sum_{l \neq k} \left(u''(r_{kl}) + \frac{2}{r_{kl}} u'(r_{kl}) \right) \right] \\ &\quad + \sum_i V_{\text{ext}}(\mathbf{r}_i) + \sum_{i < j} V_{\text{int}}(\mathbf{r}_i, \mathbf{r}_j) \end{aligned}$$

3. The Drift Force

The drift force can likewise be found by inserting the expression for the gradient (A.1) into

$$\mathbf{F}_k = 2 \frac{1}{\Psi_T(\mathbf{r})} \nabla_k \Psi_T(\mathbf{r})$$

giving

$$\begin{aligned} \mathbf{F}_k &= 2 \frac{\nabla_k \phi_k}{\phi_k} + 2 \sum_{i \neq k} \frac{\mathbf{r}_k - \mathbf{r}_i}{r_{ki}} u'(r_{kj}) \\ &= -4\alpha \left(x_k \hat{\mathbf{i}} + y_k \hat{\mathbf{j}} + \beta z_k \hat{\mathbf{k}} \right) + 2 \sum_{i \neq k} \frac{\mathbf{r}_k - \mathbf{r}_i}{r_{ki}} u'(r_{kj}) \end{aligned}$$

In the non-interactive case this reduces to

$$\mathbf{F}_k = -4\alpha \left(x_k \hat{\mathbf{i}} + y_k \hat{\mathbf{j}} + \beta z_k \hat{\mathbf{k}} \right)$$

Appendix B: Dimensionless Hamiltonian